

See discussions, stats, and author profiles for this publication at: <https://www.researchgate.net/publication/26734972>

Solution-Based Synthesis and Characterization of Cu₂ZnSnS₄ Nanocrystals

ARTICLE in JOURNAL OF THE AMERICAN CHEMICAL SOCIETY · SEPTEMBER 2009

Impact Factor: 12.11 · DOI: 10.1021/ja9044168 · Source: PubMed

CITATIONS

278

READS

454

3 AUTHORS:



Shannon C Riha

University of Wisconsin - Stevens Point

27 PUBLICATIONS 918 CITATIONS

SEE PROFILE



Bruce A Parkinson

University of Wyoming

251 PUBLICATIONS 6,901 CITATIONS

SEE PROFILE



Amy L Prieto

Colorado State University

64 PUBLICATIONS 3,199 CITATIONS

SEE PROFILE

Solution-Based Synthesis and Characterization of $\text{Cu}_2\text{ZnSnS}_4$ NanocrystalsShannon C. Riha,[†] Bruce A. Parkinson,^{*,‡} and Amy L. Prieto^{*,†}*Department of Chemistry, Colorado State University, Fort Collins, Colorado 80523, and Department of Chemistry and School of Energy Resources, University of Wyoming, Laramie, Wyoming 82071*

Received June 1, 2009; E-mail: bparkin1@uwyo.edu; Amy.Prieto@colostate.edu

Thin-film solar cells offer the promise of both low cost and scalability, features that are vital for any approach toward providing large amounts of carbon-free power.¹ CdTe and $\text{CuIn}_{1-x}\text{Ga}_x\text{Se}_2$ (CIGS) are two materials that are currently being commercialized for thin-film photovoltaic devices but may be limited in total power production by the scarcity of Te, Ga, and In.^{1–3} $\text{Cu}_2\text{ZnSnS}_4$ (CZTS) is an emerging solar cell material that contains earth-abundant elements and has a near-optimum direct band gap energy of ~ 1.5 eV and a large absorption coefficient ($>10^4 \text{ cm}^{-1}$).^{4–6} Thin-film solar cells with efficiencies of up to 5.75% have been fabricated from CZTS using costly, low-throughput sputtering and vapor deposition techniques (which are also mainly used for CdTe and CIGS production).^{1,4–6}

A new method for scaling up solar cell production is based on the synthesis of nanocrystals that are dispersed in an “ink” that can be either thermally annealed into larger-grain thin films or used to make solar cell devices using as-deposited three-dimensional arrays of photoactive nanocrystals.⁷ These approaches have spurred interest in the synthesis of ternary nanoparticles such as $\text{CuIn}(\text{S},\text{Se})_2$.^{8–10} Herein we report the synthesis of CZTS nanocrystals, the key first step in the fabrication of both nanoparticle inks and photoactive nanocrystal arrays.¹¹

We used the hot-injection solution synthesis method to prepare the CZTS nanocrystals. This method involves injecting a cold solution of precursors into a hot surfactant solution, leading to the immediate nucleation and growth of nanocrystals.^{12,13} We chose this route because it has been successful in the syntheses of a wide range of semiconducting chalcogenide nanocrystals, such as CdX ($\text{X} = \text{S}, \text{Se}, \text{Te}$) and CIGS, providing exquisite control over composition and morphology. This approach will enable low-cost fabrication of solar cell devices through techniques such as drop casting, dip coating, spin coating, or printing of the resulting CZTS nanocrystal solution.^{8,9,14–16} To our knowledge, this is the first reported synthesis of $\text{Cu}_2\text{ZnSnS}_4$ nanocrystals and the first directed synthesis of quaternary nanoparticles.

In a typical synthesis, stoichiometric amounts of copper(II) acetylacetonate, zinc acetate, and tin(IV) acetate were combined under inert conditions in oleylamine and heated to 150 °C under vacuum; the temperature was reduced to 125 °C after 0.5 h. In a separate vial, sulfur powder was sonicated in oleylamine until an orange-red solution was obtained. Trioctylphosphine oxide (TOPO) was heated to 300 °C, and the S and metal precursors were rapidly injected. Aliquots were taken every 15 min over a total reaction time of 75 min.

Figure 1 shows transmission electron microscopy (TEM) images of representative CZTS nanocrystals synthesized at 300 °C for 45 min (additional TEM images and size distribution plots for all aliquots are shown in Figure S1 in the Supporting Information).

Figure 1b is a lower-magnification TEM image of triangular and round CZTS nanocrystals with an average particle size of 12.8 ± 1.8 nm (Figure S1h). High-resolution TEM (HRTEM) (Figure 1a) shows that the nanocrystals are single-crystalline. The selected-area electron diffraction (SAED) pattern shown in Figure 1c matches the structure of CZTS (JCPDS 26-0575, indexed using the method of relative ratios), as indicated by the diffraction spots corresponding to the (112), (200), (220), (312), (008), and (332) planes. Large-area scanning electron microscopy (SEM) images show that the CZTS nanocrystals have similar sizes and pack uniformly (Figure S2a).

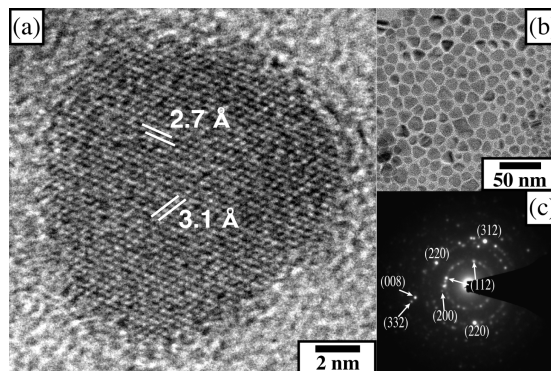


Figure 1. TEM images of $\text{Cu}_2\text{ZnSnS}_4$ nanocrystals. The HRTEM image in (a) shows interplanar spacings of 2.7 and 3.1 Å corresponding to the (200) and (112) planes, respectively; the CZTS nanocrystals in (b) have an average size of 12.8 ± 1.8 nm. The SAED pattern in (c) was indexed to CZTS.

The structure and composition of the CZTS nanocrystals were confirmed using X-ray diffraction (XRD) (Figure 2) and energy-dispersive spectroscopy (EDS) performed in both the SEM and TEM microscopes (Figures S2b and S3). The diffraction pattern shown in Figure 2 was indexed to tetragonal $\text{Cu}_2\text{ZnSnS}_4$, and the average nanocrystal size (evaluated using the Williamson–Hall method) was consistent with the particle sizes measured by TEM (Figure S4). However, the diffraction patterns of stoichiometric tetragonal Cu_2SnS_3 (JCPDS 1-089-4714) and cubic ZnS (JCPDS 5-0566) have very similar lattice parameters. EDS of various areas of the CZTS sample showed a Cu/Zn/Sn/S stoichiometric ratio of 2:1:1:4 (Figures S2b and S3). X-ray photoelectron spectroscopy (XPS) analysis was used to confirm the presence of all four elements in their expected oxidation states (Figure S5). To rule out the possibility that the samples were a coincidental stoichiometric mixture of Cu_2SnS_3 :ZnS phases, differential thermal analysis (DTA) of the nanocrystals was performed.

In the bulk, these materials all have high melting points (Cu_2SnS_3 has a phase transition at 775 °C from triclinic to cubic and melts at 850 °C;^{17,18} CZTS melts at 991 °C;¹⁸ ZnS undergoes a phase transition from cubic to wurtzite at 1020 °C and melts at 1650 °C¹⁹),

[†] Colorado State University.[‡] University of Wyoming.

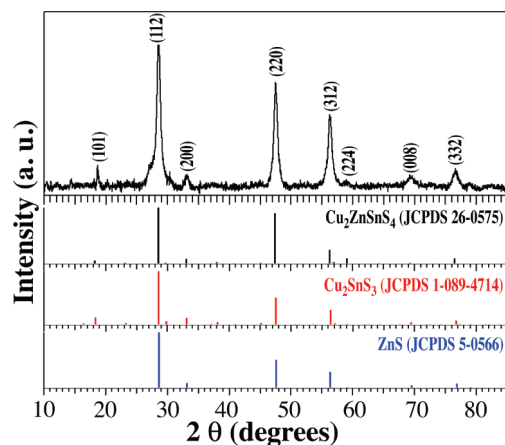


Figure 2. XRD pattern ($\lambda = 1.54 \text{ \AA}$) for the $\text{Cu}_2\text{ZnSnS}_4$ nanocrystals. The peaks have been indexed to tetragonal CZTS (JCPDS 26-0575). Below the XRD pattern are the standards for CZTS (black), CTS (red), and ZnS (blue), indicating the three materials have similar diffraction patterns.

but for nanocrystals, these temperatures could be depressed. DTA (Figure S6) of two preparations of CZTS nanocrystals, Cu_2SnS_3 nanocrystals, and a mixture of Cu_2SnS_3 and ZnS [synthesis details and XRD data for ZnS and Cu_2SnS_3 (Figure S7) are given in Supporting Information]²⁰ revealed that the two samples of CZTS each show a single phase-transition temperature below 830°C , while the Cu_2SnS_3 nanoparticles show a transition at 747°C . The mixture of Cu_2SnS_3 and ZnS exhibits two phase transitions: one at 736°C , which can be attributed to Cu_2SnS_3 , and a second at 816°C . This transition point could be attributed to either ZnS or $\text{Cu}_2\text{ZnSnS}_4$, which may have formed as the mixture was heated. The clear difference between the as-prepared CZTS samples and the intentionally mixed $\text{Cu}_2\text{SnS}_3 + \text{ZnS}$ sample indicates that the synthesized nanocrystals are pure $\text{Cu}_2\text{ZnSnS}_4$ rather than a mixture of Cu_2SnS_3 and ZnS.

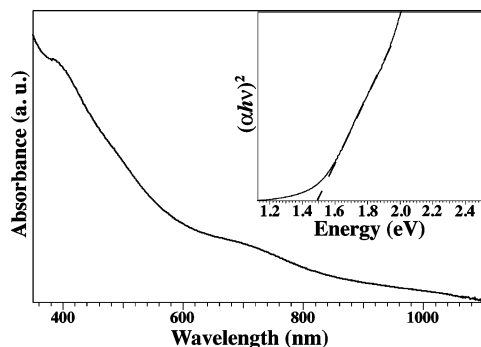


Figure 3. UV-vis absorption spectrum of $\text{Cu}_2\text{ZnSnS}_4$ nanocrystals. The inset shows an obtained band gap of 1.5 eV .

UV-vis absorption spectroscopy was used to evaluate the optical properties of the nanocrystals (Figure 3). Plotting the square of the absorption coefficient (α) multiplied by the photon energy ($h\nu$), versus $h\nu$ shows a band gap of 1.5 eV , consistent with the

literature values of $1.45\text{--}1.6 \text{ eV}$.^{4–6} This value is near the optimum for photovoltaic solar conversion in a single-band-gap device. The band gap of Cu_2SnS_3 is 0.93 eV , providing further evidence that this phase is not present.¹⁷ Preliminary experiments show that dip-cast CZTS nanocrystal films exhibit a clear photoresponse (Figure S8). An in-depth investigation of these properties will be reported shortly.²¹

We have shown for the first time that homogeneous, nearly monodisperse CZTS nanocrystals can be synthesized in solution through the hot-injection method. XRD, EDS, XPS, and DTA confirmed that the structure and composition of the as-synthesized nanocrystals correspond to those of pure $\text{Cu}_2\text{ZnSnS}_4$. UV-vis data indicate that the CZTS nanocrystals have an optical band gap of 1.5 eV , which is optimal for photovoltaic applications, and preliminary results indicate that films of these nanoparticles exhibit a clear photoresponse.

Acknowledgment. We thank Dr. John Chandler and Dr. Gary Zito at the Colorado School of Mines (HRTEM) and Dr. Sandeep Kohli at Colorado State University (DTA) for their assistance. We thank the CSU Clean Energy Supercluster and the Center for Revolutionary Solar Photoconversion (CRSP) for funding.

Supporting Information Available: Detailed information on the synthesis and characterization of $\text{Cu}_2\text{ZnSnS}_4$, Cu_2SnS_3 , and ZnS using SEM, EDS, TEM, XPS, and DTA. This material is available free of charge via the Internet at <http://pubs.acs.org>.

References

- (1) Ginley, D.; Green, M. A.; Collins, R. *MRS Bull.* **2008**, *33*, 355.
- (2) Scragg, J. J.; Dale, P. J.; Peter, L. M.; Zoppi, G.; Forbes, I. *Phys. Status Solidi B* **2008**, *245*, 1772.
- (3) Wadia, C.; Alivisatos, A. P.; Kammen, D. M. *Environ. Sci. Technol.* **2009**, *43*, 2072.
- (4) Jimbo, K.; Kimura, R.; Kamimura, T.; Yamada, S.; Maw, W. S.; Araki, H.; Oishi, K.; Katagiri, H. *Thin Solid Films* **2007**, *515*, 5997.
- (5) Katagiri, H. *Thin Solid Films* **2005**, *480*, 426.
- (6) Wadia, C.; Alivisatos, A. P.; Washio, T.; Shinohara, H.; Kurumadani, T.; Miyajima, S. *Sol. Energy Mater. Sol. Cells* **2001**, *65*, 141.
- (7) Panthani, M. G.; Akhavan, V.; Goodfellow, B.; Schmidtke, J. P.; Dunn, L.; Dodabalapur, A.; Barbara, P. F.; Korgel, B. A. *J. Am. Chem. Soc.* **2008**, *130*, 16770.
- (8) Koo, B.; Patel, R. N.; Korgel, B. A. *J. Am. Chem. Soc.* **2009**, *131*, 3134.
- (9) Tang, J.; Hinds, S.; Kelley, S. O.; Sargent, E. H. *Chem. Mater.* **2008**, *20*, 6906.
- (10) Koo, B.; Patel, R. N.; Korgel, B. A. *Chem. Mater.* **2009**, *21*, 1962.
- (11) Luther, J. M.; Law, M.; Beard, M. C.; Song, Q.; Reese, M. O.; Ellingson, R. J.; Nozik, A. J. *Nano Lett.* **2008**, *8*, 3488.
- (12) Yin, Y.; Alivisatos, A. P. *Nature* **2004**, *437*, 664.
- (13) Peng, Z. A.; Peng, X. *J. Am. Chem. Soc.* **2002**, *124*, 3343.
- (14) Cushing, B. L.; Kolesnichenko, V. L.; O'Connor, C. J. *Chem. Rev.* **2004**, *104*, 3893.
- (15) Milliron, D. J.; Hughes, S. M.; Cui, Y.; Manna, L.; Li, J.; Wang, L. W.; Alivisatos, A. P. *Nature* **2004**, *430*, 190.
- (16) Peng, X. G.; Manna, L.; Yang, W. D.; Wickman, J.; Scher, E.; Kadavanich, A.; Alivisatos, A. P. *Nature* **2000**, *404*, 59.
- (17) Fiechter, S.; Martinez, M.; Schmidt, G.; Henrion, W.; Tömm, Y. *J. Phys. Chem. Solids* **2003**, *64*, 1859.
- (18) Moh, G. H. *Chem. Erde* **1975**, *34*, 1.
- (19) Qadri, S. B.; Skelton, E. F.; Hsu, D.; Dinsmore, A. D.; Yang, J.; Gray, H. F.; Ratna, B. R. *Phys. Rev. B* **1999**, *60*, 9191.
- (20) Gu, F.; Li, C. Z.; Wang, S. F.; Lu, M. K. *Langmuir* **2006**, *22*, 1329.
- (21) Riha, S. C.; Sambur, J. B.; Liu, Y.; Parkinson, B. A.; Prieto, A. L. In preparation.

JA9044168